

# Understanding the Mechanism of B<sub>12</sub>-Dependent Methylmalonyl-CoA Mutase: Partial Proton Transfer in Action

David M. Smith,<sup>†</sup> Bernard T. Golding,<sup>‡</sup> and Leo Radom<sup>\*,†</sup>

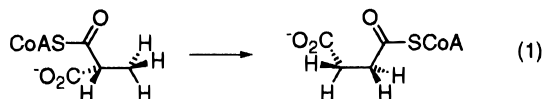
Contribution from the Research School of Chemistry, Australian National University, Canberra, ACT 0200, Australia, and Department of Chemistry, University of Newcastle upon Tyne, Newcastle upon Tyne NE1 7RU, U.K.

Received May 17, 1999

**Abstract:** Ab initio molecular orbital theory is used to investigate several possible mechanisms involving free radical intermediates for the coenzyme-B<sub>12</sub>-dependent rearrangement catalyzed by methylmalonyl-CoA mutase. Our calculations suggest that an intermolecular pathway in which transient fragmentation of the substrate-derived radical is followed by recombination of the fragments (“fragmentation–recombination”) is unlikely, but not out of the question. An alternative intramolecular pathway (“addition–elimination”) is found to be energetically more favorable. Protonation of the species involved in this latter pathway is found to further reduce the barrier for rearrangement. Examination of the middle ground between the protonated and unprotonated intramolecular mechanisms reveals a continuous spectrum of behavior and demonstrates the potential importance of partial proton transfer. Support for this proposal is obtained from the X-ray crystal structure of the protein. The stereochemistry of the rearrangement has also been examined and leads to a new proposal consistent with experiment.

## Introduction

Methylmalonyl-CoA mutase is a coenzyme-B<sub>12</sub>-dependent (adenosylcobalamin-dependent) enzyme that catalyzes the transformation of (*R*)-methylmalonyl-CoA to succinyl-CoA:



This step is the culmination of a reaction sequence in which propionyl-CoA, a toxic metabolite derived from the degradation of fats, is removed from circulation. Carboxylation of propionyl-CoA gives (*S*)-methylmalonyl-CoA, which is epimerized to (*R*)-methylmalonyl-CoA. Conversion of the (*R*)-isomer to succinyl-CoA allows further metabolism via the Krebs cycle.<sup>1</sup>

Methylmalonyl-CoA mutase is the only adenosylcobalamin-dependent enzyme known to participate in human metabolism and, as such, has received significant study. For example, several X-ray crystal structures of the enzyme obtained with various substrate analogues and inhibitors have recently appeared.<sup>2</sup> The crystal structure of an active-site mutant (Tyr89Phe) has also been solved.<sup>3</sup> These structures have revealed the mode of binding of the coenzyme, as well as providing valuable information regarding the active-site region, the binding of the

substrate, and the amino acid residues that are likely to be catalytically important.<sup>4</sup>

The mechanism of the rearrangement has been investigated since 1960, when Eggerer and co-workers<sup>5</sup> farsightedly proposed a pathway via intermediate free radicals. Subsequent investigations, aided by model studies,<sup>6</sup> have led to a number of other proposals for intermediates, including radicals, carbanions,<sup>7</sup> and organometallic species.<sup>8</sup> Support for a pathway involving organometallic intermediates comes from recent model studies whose results led to the rejection of the involvement of protein-bound free radicals in preference for a mechanism in which a crucial role is played by cobalt.<sup>9</sup> However, compelling evidence for the participation of radicals is mounting from numerous enzymatic EPR studies.<sup>10</sup> In another recent study,<sup>11</sup> a substrate-

(5) (a) Eggerer, H.; Overath, P.; Lynen, F.; Stadtman, E. R. *J. Am. Chem. Soc.* **1960**, *82*, 2643–2644. (b) Eggerer, H.; Stadtman, E. R.; Overath, P.; Lynen, F. *Biochem. Z.* **1960**, *333*, 1–9.

(6) See, for example: (a) Halpern, J. *Ann. N. Y. Acad. Sci.* **1974**, *239*, 2. (b) Tada, M.; Nakamura, N.; Matsumoto, M. *J. Am. Chem. Soc.* **1988**, *110*, 4647–4652. (c) Scott, A. I.; Karuso, P.; Williams, H. J.; Lally, J.; Robinson, J.; Nayar, G. P. *J. Am. Chem. Soc.* **1994**, *116*, 777–778. (d) Keese, R.; Dabre, T.; Arx, U. v.; Muller, S.; Wolleb-Gygi, A.; Hirschi, D.; Siljeovic, V.; Pfammatter, M.; Amolins, A.; Otten, T. In *Vitamin B<sub>12</sub> and B<sub>12</sub>-Proteins*; Krautler, B., Arigoni, D., Golding, B. T., Eds.; Wiley-VCH: Weinheim, 1998; pp 289–301.

(7) (a) Ingraham, L. L. *Ann. N. Y. Acad. Sci.* **1964**, *112*, 713–720. (b) Merkelbach, I. I.; Becht, H. G. M.; Buck, H. M. *J. Am. Chem. Soc.* **1985**, *107*, 4037–4042.

(8) (a) Pratt, J. M. *Chem. Soc. Rev.* **1985**, *14*, 161–170. (b) Choi, G.; Choi, S.; Galan, A.; Wilk, B.; Dowd, P. *Proc. Natl. Acad. Sci. U.S.A.* **1990**, *87*, 3174–3176.

(9) (a) He, M.; Dowd, P. *J. Am. Chem. Soc.* **1996**, *118*, 711. (b) He, M.; Dowd, P. *J. Am. Chem. Soc.* **1998**, *120*, 1133–1137.

(10) (a) Zhao, Y.; Such, P.; Rétey, J. *Angew. Chem., Int. Ed. Engl.* **1992**, *31*, 215–216. (b) Zhao, Y.; Abend, A.; Kunz, M.; Such, P.; Rétey, J. *Eur. J. Biochem.* **1994**, *225*, 891–896. (c) Padmakumar, R.; Banerjee, R. *J. Biol. Chem.* **1995**, *270*, 9295–9300. (d) Padmakumar, R.; Padmakumar, R.; Banerjee, R. *Biochemistry* **1997**, *36*, 3713–3718. (e) Abend, A.; Illich, V.; Rétey, J. *Eur. J. Biochem.* **1997**, *249*, 180–186.

(11) Bothe, H.; Darley, D. J.; Albracht, S. P. J.; Gerfen, G. J.; Golding, B. T.; Buckel, W. *Biochemistry* **1998**, *37*, 4105–4113.

<sup>†</sup> Australian National University.

<sup>‡</sup> University of Newcastle upon Tyne.

(1) Rétey, J. In *B<sub>12</sub>*; Dolphin, D., Ed.; J Wiley & Sons: New York, 1982; Vol. 2, pp 357–379.

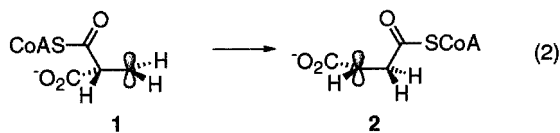
(2) (a) Mancia, F.; Keep, N. H.; Nakagawa, A.; Leadlay, P. F.; McSweeney, S.; Rasmussen, B.; Bosecke, P.; Diat, O.; Evans, P. R. *Structure* **1996**, *4*, 339–350. (b) Mancia, F.; Evans, P. R. *Structure* **1998**, *6*, 711–720.

(3) Thoma, N. H.; Meier, T. W.; Evans, P. R.; Leadlay, P. F. *Biochemistry* **1998**, *37*, 14386–14393.

(4) Ludwig, M. L.; Matthews, R. G. *Annu. Rev. Biochem.* **1997**, *66*, 269–313.

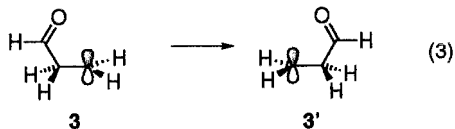
derived radical (4-glutamyl) was identified in the reaction catalyzed by the related enzyme glutamate mutase, although the nature of the other intermediates along the pathway could not be determined in this investigation. Similar studies with methylmalonyl-CoA mutase detected an organic radical but so far have been unable to make an unequivocal identification of its structure.<sup>10</sup> Free radicals have also been detected during the operation of other B<sub>12</sub>-dependent enzymes: diol dehydratase,<sup>12</sup> ribonucleotide reductase,<sup>13</sup> and ethanolamine ammonia lyase.<sup>14</sup>

It is thought that the first step in the generation of such radical species is the homolytic cleavage of the cobalt-carbon bond of the coenzyme, adenosylcobalamin.<sup>15</sup> The alkyl radical thus formed (the 5'-deoxyadenosyl radical) is proposed to abstract a hydrogen atom from the substrate to form a substrate-derived radical. Rearrangement on the radical electronic surface results in a product-related radical, which is transformed into the product by accepting a hydrogen atom from 5'-deoxyadenosine. The catalytic cycle is completed by the re-formation of the cobalt-carbon bond of the coenzyme and release of the product. The weight of experimental evidence<sup>15</sup> indicates that, if a radical mechanism were to be operative for methylmalonyl-CoA mutase, the relevant intermediates would be those shown in reaction 2.<sup>16</sup> The rearrangement thus involves a 1,2-shift of a



formyl-SCoA group to an adjacent radical center. This kind of vicinyl shift is believed to take place in the majority of the adenosylcobalamin-dependent reactions, and a general discussion of various aspects of this class of rearrangements has appeared.<sup>17</sup>

The aim of the present paper is to use high-level ab initio molecular orbital calculations to examine pathways involving possible radical intermediates relevant to the methylmalonyl-CoA mutase-catalyzed reaction. Owing to the computationally expensive nature of high-level calculations for species as large as those shown in reaction 2, our initial investigations were focused on a "model system" where the SCoA and carboxylic acid groups are replaced by hydrogen atoms. This simplification results in the degenerate rearrangement of the 3-propanal radical<sup>18</sup> (3). We have previously shown a similar approach,



when applied to the reaction catalyzed by 2-methyleneglutarate

(12) (a) Cockle, S. A.; Hill, H. A. O.; Williams, R. J. P.; Davies, S. P.; Foster, M. A. *J. Am. Chem. Soc.* **1972**, *94*, 275-276. (b) Hartmanis, M. G. N.; Stadman, T. C. *Proc. Natl. Acad. Sci. U.S.A.* **1987**, *84*, 76-79.

(13) Orme-Johnson, W. H.; Beinert, H.; Blakley, R. L. *J. Biol. Chem.* **1974**, *249*, 2338-2343.

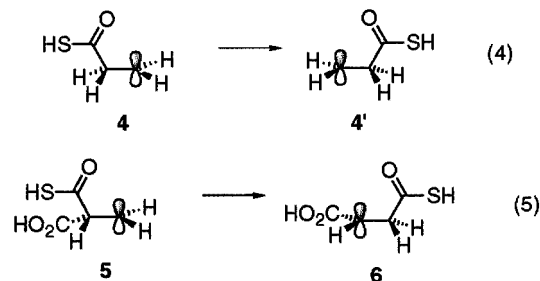
(14) Babior, B. M.; Moss, T. H.; Orme-Johnson, W. H.; Beinert, H. *J. Biol. Chem.* **1974**, *249*, 4537-4544.

(15) See, for example: (a) Rétey, J.; Robinson, J. A. In *Stereospecificity in Organic Chemistry and Enzymology*; Ebel, H. F., Ed.; Verlag Chemie: Weinheim, 1982; pp 185-207. (b) Beatrix, B.; Zelder, O.; Kroll, F. K.; Orlygsson, G.; Golding, B. T.; Buckel, W. *Angew. Chem., Int. Ed. Engl.* **1995**, *34*, 2398-2401.

(16) For a detailed discussion of the stereochemical aspects of the rearrangement, see section D.

(17) Smith, D. M.; Golding, B. T.; Radom, L. *J. Am. Chem. Soc.* **1999**, *121*, 1037-1044.

mutase, to be a useful approximation.<sup>17</sup> To further check the validity of our model and to investigate the incremental effects of the additional substituents, we also performed calculations on the more complete model systems shown in reactions 4 and 5.



Kinetic measurements on the protein show that the rate constant for the overall reaction (in the direction shown in eq 1) is  $k_{\text{cat}} = 48.3 \text{ s}^{-1}$ .<sup>19</sup> Using a method suggested by George et al.,<sup>20</sup> we find that the barrier for the rate-limiting step should lie between approximately 60 and 75 kJ mol<sup>-1</sup> at 37 °C. Furthermore, experiments with <sup>3</sup>H-labeled adenosylcobalamin that measured the partitioning of the released tritium between the substrate and product indicate that the radical rearrangement step is not kinetically significant.<sup>19</sup> That is, a rapid equilibrium is established between the substrate-derived and product-related radicals (eq 2), and the rate-limiting step is likely to be either hydrogen abstraction or product release. This information, taken together with the estimated barrier noted above for the overall reaction, suggests that the activation required for the radical rearrangement should be quite low (at least less than about 60 kJ mol<sup>-1</sup>). In this paper, we investigate possible mechanisms for the radical rearrangement in an attempt to reveal likely pathways and to shed some light on how the protein might lower the barrier for this intrinsically difficult reaction step. Due to the highly reactive nature of the radical species involved, this is a problem ideally suited to a computational approach.<sup>21</sup>

## Theoretical Procedures

Standard ab initio molecular orbital calculations<sup>22</sup> were performed with GAUSSIAN 94,<sup>23</sup> GAUSSIAN 98,<sup>24</sup> and MOLPRO 97.<sup>25</sup> In the present work, unlike our other closely related studies,<sup>17,26</sup> we have used the B3-LYP/6-31G(d,p) (rather than B3-LYP/6-31G(d)) procedure for the generation of geometries and zero-point vibrational energies. This modification was employed primarily to provide an improved description of the hydrogen-bonded complexes reported herein, but for consistency it was also maintained throughout the remainder of the

(18) For simplicity, we have referred to structure 3 (<sup>•</sup>CH<sub>2</sub>CH<sub>2</sub>CHO) as the 3-propanal radical. This species may be better named as the 3-oxoprop-1-yl radical. Similarly, we have referred to 1 as the methylmalonyl-CoA-derived radical, 5 as the methylmalonyl-derived radical, 2 as the succinyl-CoA-related radical, and 6 as the succinyl-related radical.

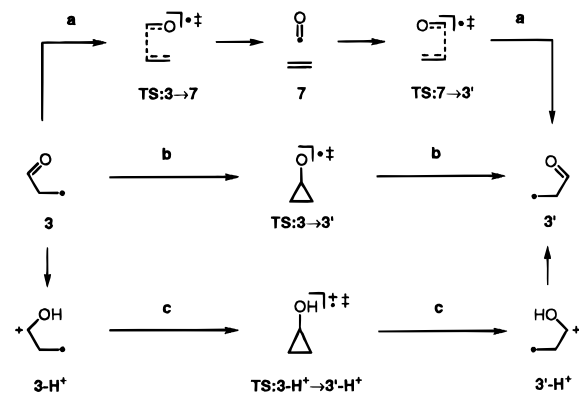
(19) Meier, T. W.; Thoma, N. H.; Leadlay, P. F. *Biochemistry* **1996**, *35*, 11791-11796.

(20) George, P.; Glusker, J. P.; Bock, C. W. *J. Am. Chem. Soc.* **1997**, *119*, 7065-7074.

(21) A preliminary account of this work has appeared: Smith, D. M.; Golding, B. T.; Radom, L. *J. Am. Chem. Soc.* **1999**, *121*, 1383-1384.

(22) Hehre, W. J.; Radom, L.; Schleyer, P. v. R.; Pople, J. A. *Ab Initio Molecular Orbital Theory*; Wiley: New York, 1986.

(23) Frisch, M. J.; Trucks, G. W.; Schlegel, H. B.; Gill, P. M. W.; Johnson, B. G.; Robb, M. A.; Cheeseman, J. R.; Keith, T.; Petersson, G. A.; Montgomery, J. A.; Raghavachari, K.; Al-Laham, M. A.; Zakrzewski, V. G.; Ortiz, J. V.; Foresman, J. B.; Cioslowski, J.; Stefanov, B. B.; Nanayakkara, A.; Challacombe, M.; Peng, C. Y.; Ayala, P. Y.; Chen, W.; Wong, M. W.; Andres, J. L.; Replogle, E. S.; Gomperts, R.; Martin, R. L.; Fox, D. J.; Binkley, J. S.; Defrees, D. J.; Baker, J.; Stewart, J. P.; Head-Gordon, M.; Gonzalez, C.; Pople, J. A. *Gaussian 94*, Revision E.2; Gaussian, Inc.: Pittsburgh, PA, 1995.

**Scheme 1.** Possible Mechanisms for the Degenerate Rearrangement of the 3-Propanal Radical (**3**)

study. Improved relative energies were obtained from two modified compound methods that have been shown to perform well for free radicals. The first of these (referred to as CBS-RAD(p)) is essentially the same as the previously employed<sup>17,26</sup> CBS-RAD(B3-LYP,B3-LYP)<sup>27</sup> technique, except for the addition of polarization functions on hydrogen atoms during the geometry and frequency calculations.<sup>28</sup> The CBS-RAD methodology has been shown to perform well for the related ring opening of the cyclopropylcarbinyl radical<sup>26</sup> as well as for a variety of radical additions to alkenes.<sup>29</sup> As the computationally most expensive of the techniques employed in this study, the CBS-RAD(p) calculations were feasible only for the systems shown in reactions 3 and 4. For the larger system shown in reaction 5 (and also for reactions 3 and 4 for the sake of comparison), we employed a slightly modified version of the G2(MP2,SVP)-RAD(B3-LYP)<sup>30</sup> technique (henceforth referred to as G2(MP2,SVP)-RAD(p)). The parent method (without polarization functions on hydrogen during the geometry and frequency calculations) has recently been shown to perform well for a range of radical stabilization energies.<sup>30</sup> The presently employed variant (G2(MP2,SVP)-RAD(p)) demonstrates impressive agreement with CBS-RAD(p) in the current study as well as in a closely related investigation of the diol dehydratase-catalyzed reactions.<sup>31</sup> We have also presented the B3-LYP/6-31G(d,p) energies for comparison. Unless otherwise noted, relative energies in the text refer to CBS-RAD(p) values for the species involved in reactions 3 and 4 and G2(MP2,SVP)-RAD(p) values for the species involved in reaction 5, in both cases at 0 K. All structural values quoted

(24) Frisch, M. J.; Trucks, G. W.; Schlegel, H. B.; Scuseria, G. E.; Robb, M. A.; Cheeseman, J. R.; Zakrzewski, V. G.; Montgomery, J. A., Jr.; Stratmann, R. E.; Burant, J. C.; Dapprich, S.; Millam, J. M.; Daniels, A. D.; Kudin, K. N.; Strain, M. C.; Farkas, O.; Tomasi, J.; Barone, V.; Cossi, M.; Cammi, R.; Mennucci, B.; Pomelli, C.; Adamo, C.; Clifford, S.; Ochterski, J.; Petersson, G. A.; Ayala, P. Y.; Cui, Q.; Morokuma, K.; Malick, D. K.; Rabuck, A. D.; Raghavachari, K.; Foresman, J. B.; Cioslowski, J.; Ortiz, J. V.; Stefanov, B. B.; Liu, G.; Liashenko, A.; Piskorz, P.; Komaromi, I.; Gomperts, R.; Martin, R. L.; Fox, D. J.; Keith, T.; Al-Laham, M. A.; Peng, C. Y.; Nanayakkara, A.; Gonzalez, C.; Challacombe, M.; Gill, P. M. W.; Johnson, B.; Chen, W.; Wong, M. W.; Andres, J. L.; Gonzalez, C.; Head-Gordon, M.; Replogle, E. S.; Pople, J. A. *Gaussian 98*, Revision A.6; Gaussian, Inc.: Pittsburgh, PA, 1998.

(25) MOLPRO 97 is a package of ab initio programs written by H.-J. Werner and P. J. Knowles, with contributions from J. Almlöf, R. D. Amos, A. Berning, D. L. Cooper, M. J. O. Deegan, A. J. Dobbyn, F. Eckert, S. T. Elbert, C. Hampel, R. Lindh, W. A. Lloyd, W. Meyer, A. Nickless, K. Peterson, R. Pitzer, A. J. Stone, P. R. Taylor, M. E. Mura, P. Pulay, M. Schütz, H. Stoll, and T. Thorsteinsson.

(26) Smith, D. M.; Nicolaidis, A.; Golding, B. T.; Radom, L. *J. Am. Chem. Soc.* **1998**, *120*, 10223–10233.

(27) Mayer, P. M.; Parkinson, C. J.; Smith, D. M.; Radom, L. *J. Chem. Phys.* **1998**, *108*, 604–615.

(28) The maximum difference obtained between CBS-RAD and CBS-RAD(p) relative energies for the rearrangement shown in reaction 3 is 0.9 kJ mol<sup>-1</sup>.

(29) Wong, M. W.; Radom, L. *J. Phys. Chem.* **1998**, *102*, 2237–2245.

(30) (a) Parkinson, C. J.; Mayer, P. M.; Radom, L. *Theor. Chim. Acta* **1999**, *102*, 92–96. (b) Parkinson, C. J.; Mayer, P. M.; Radom, L. Work in progress. (c) Parkinson, C. J.; Radom, L. Work in progress.

(31) Smith, D. M.; Golding, B. T.; Radom, L. *J. Am. Chem. Soc.* **1999**, *121*, 5700–5704.

**Table 1.** Relative Energies (kJ mol<sup>-1</sup>)<sup>a</sup> of the Species Involved in the Degenerate Rearrangement of the 3-Propanal Radical (**3**) at 0 K

	CBS-RAD(p)	G2(MP2,SVP)-RAD(p)	B3-LYP/6-31G(d,p)
3-propanal radical ( <b>3</b> )	0.0	0.0	0.0
TS: <b>3</b> → <b>7</b>	93.2	96.1	90.2
formyl radical + ethylene ( <b>7</b> )	66.9	63.6	72.2
TS: <b>3</b> → <b>3'</b>	46.9	51.8	39.8
protonated 3-propanal radical ( <b>3</b> -H <sup>+</sup> )	0.0	0.0	0.0
TS: <b>3</b> -H <sup>+</sup> → <b>3'</b> -H <sup>+</sup>	10.0	12.7	13.0
<b>3</b> -NH <sub>4</sub> <sup>+</sup>	0.0	0.0	0.0
TS: <b>3</b> -NH <sub>4</sub> <sup>+</sup> → <b>3'</b> -NH <sub>4</sub> <sup>+</sup>	24.5	21.9	20.2
proton affinity of <b>3</b>	788.2	787.7	820.4
proton affinity of TS: <b>3</b> → <b>3'</b>	825.1	826.8	847.2

<sup>a</sup> Energies relative to either **3**, **3**-H<sup>+</sup>, or **3**-NH<sub>4</sub><sup>+</sup>.

are derived from the B3-LYP/6-31G(d,p)-optimized geometries. Calculated CBS-RAD(p) and G2(MP2,SVP)-RAD(p) total energies and GAUSSIAN 94 and GAUSSIAN 98 archive entries for the B3-LYP/6-31G(d,p)-optimized geometries for all relevant structures are presented in Tables S1–S4 of the Supporting Information.

## Results and Discussion

### A. Degenerate Rearrangement of the 3-Propanal Radical

(**3**). We investigated three distinct mechanistic possibilities (see Scheme 1) for the rearrangement shown in reaction 3.<sup>32</sup> The first of these (pathway a) involves a homolytic bond fission in **3** to give the formyl radical plus ethylene (collectively referred to as **7**), followed by an intermolecular radical addition to form the rearranged product **3'**. Fragmentation–recombination mechanisms of this kind have been recently suggested to provide a possible unifying hypothesis for the B<sub>12</sub>-dependent carbon skeleton mutases.<sup>15b</sup> As was the case in the degenerate rearrangement of the but-3-enyl radical,<sup>17</sup> we find the fragmentation–recombination pathway for reaction 3 to be associated with a relatively high barrier (93.2 kJ mol<sup>-1</sup>, see Table 1 and Figure 1). The separated fragments (**7**) are found to lie 26.3 kJ mol<sup>-1</sup> lower than the transition structure (TS:**3**→**7**) or 66.9 kJ mol<sup>-1</sup> above the reactant (**3**).

The second possible pathway (Scheme 1, route b) involves an intramolecular migration of the formyl group in what is commonly thought of as a two-step process. The first step involves an intramolecular radical addition to the carbonyl carbon to form an intermediate cyclopropyloxy radical (shown in Scheme 1 as TS:**3**→**3'**). The three-membered ring can then undergo a ring-opening elimination reaction to give the desired product,<sup>33</sup> and hence this pathway is sometimes referred to as the addition–elimination mechanism. We find that the cyclopropyloxy radical lies in a very shallow well (with a depth of 0.3 kJ mol<sup>-1</sup>) on the electronic potential energy surface, which is found to disappear upon the inclusion of zero-point vibrational energy. We therefore conclude that the cyclopropyloxy radical does not correspond to a stable intermediate and that the addition–elimination pathway is essentially a single-step process

(32) Of the several stable conformers of the 3-propanal radical, the lowest-energy form has C<sub>s</sub> symmetry, with one of the methylene hydrogens associated with the radical center participating in an intramolecular hydrogen bond with the carbonyl oxygen. Slightly higher in energy (by 2.9 kJ mol<sup>-1</sup>) is a conformer with C<sub>1</sub> symmetry, shown in Figure 2. The global minimum on the surface associated with protonation has such a C<sub>1</sub> conformation (also included in Figure 2). To avoid conformational complications in the comparison of protonated and non-protonated pathways, we have used this C<sub>1</sub> conformation for energetic comparisons involving the 3-propanal radical. We note that the X-ray crystal structures (see section E) indicate that the C<sub>1</sub> structure is the one that most closely resembles the bound conformation of the substrate.

(33) Giese, B.; Horler, H. *Tetrahedron Lett.* **1983**, *24*, 3221–3224.



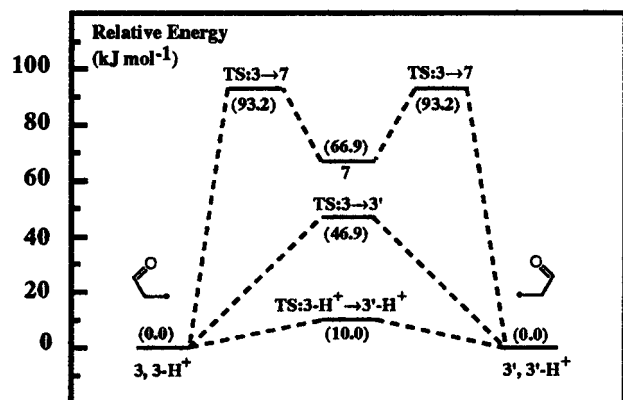


**Figure 1.** Schematic CBS-RAD(p) energy profile for the degenerate rearrangement of the 3-propanal radical (3). Relative energies ( $\text{kJ mol}^{-1}$ ) are shown in parentheses.

(as shown in Figure 1). Nevertheless, the barrier for this intramolecular rearrangement ( $46.9 \text{ kJ mol}^{-1}$ , see Table 1)<sup>34</sup> is considerably lower than that calculated for the fragmentation–recombination pathway.

Encouraged by the results of previous calculations which showed the beneficial effects of protonation in facilitating 1,2-shifts in other free radicals,<sup>17,31,35</sup> and following the specific suggestion of protonating the migrating carbonyl group,<sup>35</sup> we investigated the protonated 3-propanal radical ( $3\text{-H}^+$ ).<sup>36</sup> The resulting 1,2-shift of the CHOH group (Scheme 1, pathway c) is found to proceed, via a single transition structure, with an extremely low barrier ( $10.0 \text{ kJ mol}^{-1}$ ).<sup>37</sup> We believe that this result is particularly important in understanding how methylmalonyl-CoA mutase catalyzes the interconversion of the substrate-derived and product-related radicals.

It is also of interest to briefly consider the effects of protonation on the fragmentation–recombination pathway. In the extreme case of a fully protonated substrate in the gas phase, the separated fragments (the protonated formyl radical plus ethylene) are found to lie some  $258.8 \text{ kJ mol}^{-1}$  above the protonated propanal radical, with no simple fragmentation–recombination pathway evident. This high calculated energy can be taken to imply that the introduction of a charge (via the interaction of a proton) qualitatively disfavors the fragmentation–recombination mechanism.

Table 1 shows the energetics of the three pathways from Scheme 1 (as well as one additional pathway, see below). We find the results from the CBS-RAD(p) and G2(MP2,SVP)-RAD(p) techniques to be in good agreement with one another. The much less expensive B3-LYP/6-31G(d,p) density functional method also fares quite well in comparison with its computationally more elaborate counterparts.

(34) The quoted barrier corresponds to the energy of the symmetrical structure, which, after inclusion of the zero-point energy, is higher than the two nonsymmetrical transition structures (see Supporting Information).

(35) (a) Golding, B. T.; Radom, L. *J. Chem. Soc., Chem. Commun.* **1973**, 939–941. (b) Golding, B. T.; Radom, L. *J. Am. Chem. Soc.* **1976**, *98*, 6331–6338.

(36) The additional proton can be either syn or anti to the carbon framework. The lowest-energy arrangement is the anti form (shown in Figure 2). The X-ray crystal structures (section E) suggest that, if a proton were to interact with the carbonyl oxygen, then it would do so from the face of the molecule consistent with this conformation. For reasons of consistency and biological relevance, we have maintained this arrangement for all subsequent examples involving protonation of the carbonyl group throughout this paper.

(37) This same shift has been investigated previously in the context of mass spectrometry experiments using lower-level molecular orbital calculations and mass spectrometry.<sup>38</sup>

(38) Bouchoux, G.; Luna, A.; Tortajada, J. *Int. J. Mass Spectrom. Ion Processes* **1997**, *167/168*, 353–374.

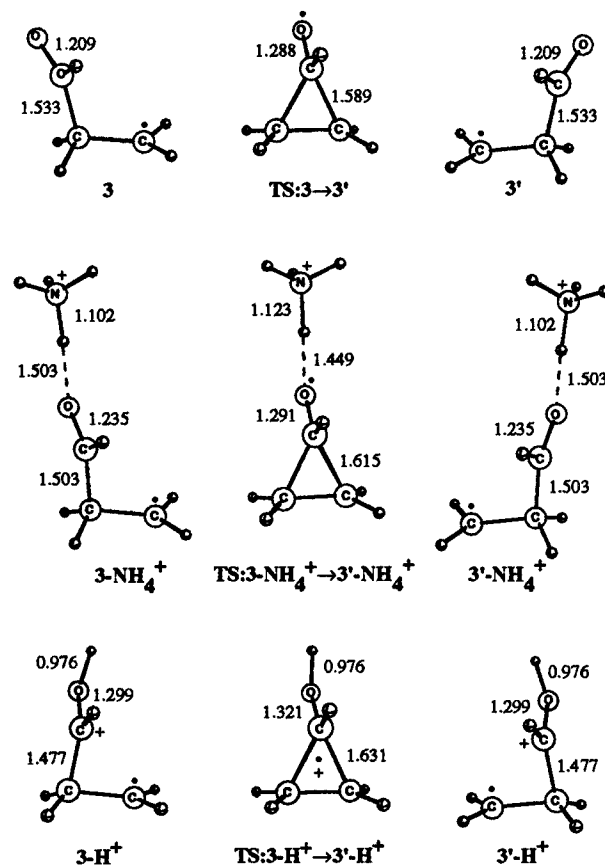


**Figure 2.** B3-LYP/6-31G(d,p) structures and selected bond lengths ( $\text{\AA}$ ) for the species involved in the rearrangement of the unprotonated (3), partially protonated ( $3\text{-NH}_4^+$ ), and fully protonated ( $3\text{-H}^+$ ) 3-propanal radical.

**B. Partial-Proton-Transfer Concept.** Our results for the rearrangement of the 3-propanal radical suggest that protonation of the thioester group would facilitate the rearrangement. However, the concept of substrate protonation, while energetically attractive, carries with it the problem that it is difficult to achieve substantial protonation of a weak base with the weakly acidic groups available to enzymes.<sup>39</sup> Thus, the  $\text{p}K_a$  of the conjugate acid of a thioester carbonyl oxygen is estimated to be around  $-6$ ,<sup>40</sup> so even the strongest conceivable acid in a protein cannot be expected to generate a substantial concentration of protonated substrate.

Owing to the problems associated with mechanisms involving full protonation, we have considered whether *partial proton transfer* would be sufficient to activate the formyl group to migrate.<sup>21</sup> To investigate such behavior, we initially examined the interaction of the 3-propanal radical with a representative acid ( $\text{NH}_4^+$ ). Figure 2 shows structures and representative bond lengths of the rearranging 3-propanal radical ( $3 \rightarrow 3'$ ), species involved in the fully protonated rearrangement ( $3\text{-H}^+ \rightarrow 3'\text{-H}^+$ ), and the system in the presence of ammonium ( $3\text{-NH}_4^+ \rightarrow 3'\text{-NH}_4^+$ ). From a structural perspective, the interaction of ammonium can be seen to represent a situation intermediate between the extremes of full and no protonation. In particular, this intermediacy is evident from the changes in the  $\text{C}=\text{O}$  bond length upon progressing from one extreme to the other. Furthermore, the  $\text{N}-\text{H}$  bond in isolated ammonium ( $1.027 \text{ \AA}$ ) is found to be significantly extended ( $1.102 \text{ \AA}$ ) upon interaction

(39) Thibblin, A.; Jencks, W. P. *J. Am. Chem. Soc.* **1979**, *101*, 4963–4973.

(40) Edward, J. T.; Wong, S. C.; Welch, G. *Can. J. Chem.* **1978**, *59*, 931–940.

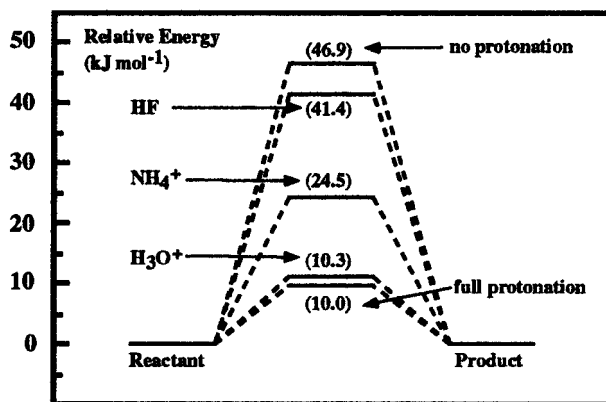


**Figure 3.** Schematic CBS-RAD(p) energy profile for the rearrangement of the 3-propanal radical (**3**), showing barriers ( $\text{kJ mol}^{-1}$ ) associated with various degrees of protonation.

with the carbonyl oxygen, a change that suggests partial transfer of the proton.

To show that ammonium is not an isolated example and that there is actually a continuum of behavior between the two extremes, we extended our acid set to include a stronger ( $\text{H}_3\text{O}^+$ ) and a weaker (HF) proton donor. This choice encompasses a wide range of acid strengths, as measured by the proton affinities (PAs) of the conjugate bases ( $F^- = 1556.0$ ,  $\text{NH}_3 = 848.6$ , and  $\text{H}_2\text{O} = 680.1 \text{ kJ mol}^{-1}$ ).<sup>41</sup> The distance between the acidic proton and the carbonyl oxygen of the 3-propanal radical in the relevant complexes is the most direct measure of the degree of proton transfer to oxygen. We find that this distance decreases across the acid series from infinity (no protonation) to 1.727 (HF), 1.503 ( $\text{NH}_4^+$ ), 1.046 ( $\text{H}_3\text{O}^+$ ), and 0.976 Å (full protonation). A similar trend (but in the opposite direction) is found for the C=O bond, with HF causing a slight lengthening to 1.221 Å, while  $\text{H}_3\text{O}^+$  imparts a larger effect with a calculated carbonyl bond length of 1.273 Å. This same monotonic trend can be found for several of the other geometric parameters.

The most striking consequence of the transition from non-protonation to complete protonation of the carbonyl group of the 3-propanal radical is the monotonic lowering of the barrier to migration of the formyl group (see Figure 3).<sup>42</sup> As might have been expected from the barriers in the extreme cases (Figure 1 and Table 1), a greater degree of proton transfer is associated with a lower barrier to rearrangement. The acidity of  $\text{H}_3\text{O}^+$  is sufficient to result in a barrier ( $10.3 \text{ kJ mol}^{-1}$ ) virtually identical to that calculated for full protonation, while the barrier with HF as the acid ( $41.4 \text{ kJ mol}^{-1}$ ) shows that even a small amount of proton transfer can result in a significant decrease in the barrier for migration. With the ammonium ion, the moderately high proton affinity of ammonia maintains the relatively strong binding of the proton while allowing sufficient proton transfer to facilitate the rearrangement, to the extent that the barrier is reduced to  $24.5 \text{ kJ mol}^{-1}$ . In the context of enzymatic catalysis, this situation might be regarded as ideal since significant barrier lowering can be achieved without deprotonation of the enzyme.

(41) These species, although not physiologically significant themselves, were chosen to demonstrate how the migration behavior depends on the strength of the interacting acid. On this basis, the amino acids His- $\text{H}^+$  and Lys- $\text{H}^+$  could be expected to show behavior similar to that of  $\text{NH}_4^+$ , while Asp and Glu should be closer to  $\text{H}_3\text{O}^+$ , and Cys and Tyr closer to HF.

(42) The rearrangement assisted by HF has the same electronic profile as the uncatalyzed pathway.<sup>34</sup> That is, the symmetrical structure (whose energy is shown in Figure 3) corresponds to a minimum on the vibrationless potential energy surface that disappears upon inclusion of zero-point energy. With either  $\text{NH}_4^+$  or  $\text{H}_3\text{O}^+$  as the acid, the symmetrical species is a transition structure on the vibrationless surface.

It is possible to phrase the partial-proton-transfer concept in the same language of hydrogen bonding that has been employed in the current debate over whether “low-barrier” hydrogen bonds (LBHBs) or “short strong” hydrogen bonds (SSHBs) can be important in enzymatic catalysis.<sup>43</sup> The discussion has focused on concepts such as the  $\text{pK}_a$  matching of the H-bonding donor and acceptor,<sup>44</sup> the positioning of the shared proton,<sup>45</sup> the distance between the donor and acceptor atoms,<sup>46</sup> the strength of the hydrogen bond,<sup>47</sup> and the nonexistence of SSHBs under certain solvation conditions.<sup>48</sup> We believe that our results and their interpretation make an important contribution to this debate, for it is conceptually instructive to examine the “low-barrier” hydrogen-bonding hypothesis in terms of partial proton transfers.

The lowering of a reaction barrier by protonation is equivalent to saying that the transition structure interacts more favorably with the proton than does the reactant. For example, the energy of the transition structure (**TS:3-3'**) is lowered by  $825.1 \text{ kJ mol}^{-1}$  upon protonation, while the 3-propanal radical (**3**) has a proton affinity of  $788.2 \text{ kJ mol}^{-1}$  (Table 1). The difference between these two energies of  $36.9 \text{ kJ mol}^{-1}$  is exactly the reduction in barrier associated with protonation. The same concept applies to partial protonation. That is, the gas-phase hydrogen bond between the 3-propanal radical and  $\text{NH}_4^+$  is quite strong ( $96.9 \text{ kJ mol}^{-1}$ ), despite the fact that the proton transfer between donor and acceptor is described by a *single, asymmetric* energy well. However, the  $22.3 \text{ kJ mol}^{-1}$  lowering of the rearrangement barrier (corresponding to a rate increase of ca. 5 orders of magnitude) by  $\text{NH}_4^+$  comes not from the strength of this hydrogen bond but from the fact that the interaction between  $\text{NH}_4^+$  and the transition structure ( $119.2 \text{ kJ mol}^{-1}$ ) is  $22.3 \text{ kJ mol}^{-1}$  stronger than its interaction with the reactant, due to the higher “proton affinity” of the former species. This concept is also evident from the geometric parameters shown in Figure 2, in that the degree of proton transfer to the transition structure is clearly greater than it is to the reactant.

In an enzymatic reaction facilitated by protonation, the proton-accepting site will generally carry some small amount of negative charge, making it a good candidate for binding to a proton donor in the protein via a hydrogen bond. If such a hydrogen bond exists and remains intact during the course of the reaction, then, regardless of the strength of the H bond donor, the barrier will be lowered simply because the transition structure interacts more strongly with the proton than does the substrate. Enzymes may therefore utilize substrate hydrogen bonding for both binding *and* catalysis. The transition from a “weak” hydrogen bond to a “short strong” hydrogen bond is

(43) (a) Gerlt, J. A.; Gassman, P. G. *J. Am. Chem. Soc.* **1993**, *115*, 11552–11568. (b) Cleland, W. W.; Kreevoy, M. M. *Science* **1994**, *264*, 1887–1890. (c) Frey, P. A.; Whitt, S. A.; Tobin, J. B. *Science* **1994**, *264*, 1927–1930.

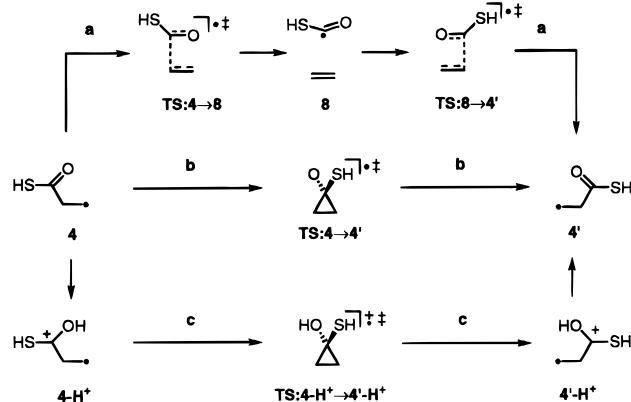
(44) (a) Scheiner, S.; Kar, T. *J. Am. Chem. Soc.* **1995**, *117*, 6970–6975. (b) Shan, S.; Loh, S.; Herschlag, D. *Science* **1996**, *272*, 97–101. (c) Garcia-Viloca, M.; Gonzalez-Lafont, A.; Lluch, J. M. *J. Phys. Chem. A* **1997**, *101*, 3880–3886.

(45) (a) Perrin, C. L.; Nielson, J. B. *Annu. Rev. Phys. Chem.* **1997**, *48*, 511–544. (b) Tuckerman, M. E.; Marx, D.; Klein, M. L.; Parrinello, M. *Science* **1997**, *275*, 817–820. (c) Ash, E. L.; Sudmeier, J. L.; DeFabo, E. C.; Bachovchin, W. W. *Science* **1997**, *278*, 1128–1132. (d) Perrin, C. L.; Nielson, J. B.; Kim, Y. *Ber. Bunsen-Ges. Phys. Chem.* **1998**, *102*, 403–409.

(46) Gilli, P.; Bertolasi, V.; Ferretti, V.; Gilli, G. *J. Am. Chem. Soc.* **1994**, *116*, 909–915.

(47) (a) Guthrie, J. P. *Chem. Biol.* **1996**, *3*, 163–170. (b) Pan, Y.; McAllister, M. J. *Am. Chem. Soc.* **1997**, *119*, 7561–7566. (c) Pan, Y.; McAllister, M. J. *Am. Chem. Soc.* **1998**, *120*, 166–169.

(48) (a) Warshel, A.; Papazyan, A.; Kollman, P. A. *Science* **1995**, *269*, 102–103. (b) Warshel, A.; Papazyan, A. *Proc. Natl. Acad. Sci. U.S.A.* **1996**, *93*, 13665–13670.

**Scheme 2.** Possible Mechanisms for the Degenerate Rearrangement of the 1-Sulfanyl-3-propanal Radical (4)

continuous, and, regardless of where a particular H-bonding interaction happens to lie on this scale, there will be a contribution to the lowering of the barrier made by partial proton transfer. Our thesis is simple: *any reaction that is facilitated by protonation will also be facilitated (to a moderated extent) by the partial proton transfer that enzymatic hydrogen bonding can provide.*

It is unlikely that a given partial proton transfer would be overly efficient in aqueous solution. In much the same way as has been argued in the context of the LBHB hypothesis,<sup>48b</sup> the hydrogen-bonding donor/acceptor properties of water and the entropic disorder associated with such a solution are likely to disrupt the hydrogen bond. However, the active sites of many enzymes are sequestered from bulk water, at least to some extent, and may, therefore, provide an environment well suited to hydrogen bonding somewhat undisturbed by solvent. In particular, the active site of methylmalonyl-CoA mutase has been shown to be deeply buried and largely inaccessible to solvent<sup>2a</sup> (see section E), seemingly providing such a tailored environment. Furthermore, the X-ray crystal structures<sup>2,3</sup> indicate that an active-site histidine residue (His244, see section E) is in a position to bind the carbonyl oxygen of the substrate by means of a hydrogen bond. We suggest that this hydrogen bond not only serves to bind the substrate but also provides partial proton transfer for catalysis. In this way, the enzyme can take advantage of the proton-induced barrier lowering that is available for the intramolecular rearrangement, without resorting to the extreme of full protonation.<sup>49</sup>

The fragmentation–recombination rearrangement (pathway a, Scheme 1) is a reaction that is seemingly disfavored by protonation. Extrapolation of the partial-proton-transfer concept to this example would suggest that the presence of a hydrogen bond donor in close proximity to the carbonyl oxygen would not be favorable for this pathway.

**C. Degenerate Rearrangement of the 1-Sulfanyl-3-propanal Radical (4).** To ascertain the effect of the sulfanyl group on the rearrangement, we investigated the reactions of the 1-sulfanyl-3-propanal radical (4, see Scheme 2).<sup>50</sup> Sulfanyl substitution is found to lower the barrier for the fragmentation–recombination (pathway a) to 84.1 kJ mol<sup>-1</sup>, with the separated

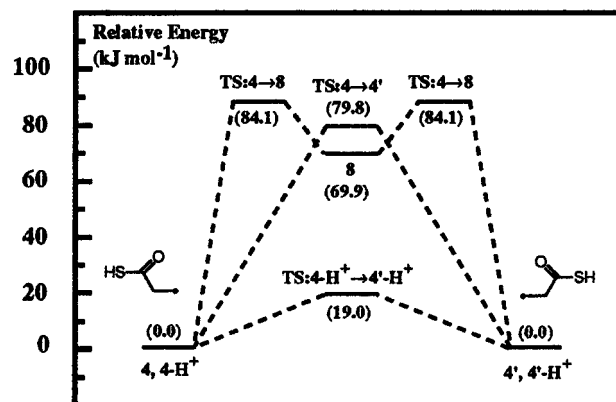
(49) The enolization step of citrate synthase could also be described in terms of partial proton transfer. See, for example: Mulholland, A. J.; Richards, W. G. *J. Phys. Chem. B* **1998**, *102*, 6635–6646.

(50) The lowest-energy conformation of the 1-sulfanyl-3-propanal radical (4) has C<sub>s</sub> symmetry, with the sulfur lone pair directly above the perpendicular radical center. For the same reasons as discussed for the parent 3-propanal radical,<sup>32</sup> we have used the slightly higher energy C<sub>1</sub> conformer for our calculations involving this molecule.

**Table 2.** Relative Energies (kJ mol<sup>-1</sup>)<sup>a</sup> of the Species Involved in the Degenerate Rearrangement of the 1-Sulfanyl-3-propanal Radical (4) at 0 K

	CBS-RAD(p)	G2(MP2,SVP)-RAD(p)	B3-LYP/6-31G(d,p)
1-sulfanyl-3-propanal radical (4)	0.0	0.0	0.0
TS:4→8	84.1	88.3	82.7
sulfanylformyl radical + ethylene (8)	69.9	66.6	67.7
TS:4→4'	79.8	81.3	75.2
4-H <sup>+</sup>	0.0	0.0	0.0
TS:4-H <sup>+</sup> →4'-H <sup>+</sup>	19.0	27.7	26.2
4-NH <sub>4</sub> <sup>+</sup>		0.0	0.0
TS:4-NH <sub>4</sub> <sup>+</sup> →4'-NH <sub>4</sub> <sup>+</sup>		63.5	55.6
proton affinity of 4	789.1	792.2	808.9
proton affinity of TS:4→4'	850.1	845.8	857.7

<sup>a</sup> Energies relative to either 4, 4-H<sup>+</sup>, or 4-NH<sub>4</sub><sup>+</sup>.

**Figure 4.** Schematic CBS-RAD(p) energy profile for the degenerate rearrangement of the 1-sulfanyl-3-propanal radical (4). Relative energies (kJ mol<sup>-1</sup>) are shown in parentheses.

fragments (the sulfanylformyl radical plus ethylene, collectively referred to as 8) lying 69.9 kJ mol<sup>-1</sup> above the reactant (see Table 2). The 1-sulfanyl-cyclopropoxy radical is found to be not a stable intermediate but rather a transition structure (TS:4→4') describing the intramolecular 1,2-shift of the COSH group (pathway b). The migration barrier associated with this transition structure is found to be 79.8 kJ mol<sup>-1</sup>. A schematic energy profile for these pathways (along with pathway c) can be found in Figure 4.

The proton affinity of the 1-sulfanyl-3-propanal radical (4) is calculated to be 789.1 kJ mol<sup>-1</sup>,<sup>51</sup> almost identical to that of

(51) We have assigned the conformer of the protonated 1-sulfanyl-3-propanal radical (4-H<sup>+</sup>), with both protons anti to the carbon framework as the zero of energy on this surface<sup>36</sup> (and the proton affinity is thus defined with respect to this structure). A C<sub>1</sub> transition structure (at 18.8 kJ mol<sup>-1</sup>) is found that connects this conformer with a structure (at -2.8 kJ mol<sup>-1</sup>) that has undergone the 1,2-shift of the CSHOH group but has the thiolic proton in a syn arrangement with respect to the carbon framework. A mirror image of this transition structure describes an analogous CSHOH migration. These two enantiomeric transition structures are connected by a second-order saddle point of C<sub>s</sub> symmetry (TS:4-H<sup>+</sup>→4'-H<sup>+</sup> at 19.0 kJ mol<sup>-1</sup>) that is only marginally higher in energy than the two nonsymmetrical first-order saddle points. Traversing this C<sub>s</sub> structure provides one means for the 1,2-shift to occur with both protons remaining anti to the ring. There may, however, be a lower-energy pathway connecting the two C<sub>1</sub> transition structures, implying that the barrier that incorporates the C<sub>s</sub> structure can be viewed as an upper bound for the overall migration process. Our reported data on the 1,2-shift (including the “proton affinity” of the unprotonated transition structure) are thus calculated using this symmetrical, second-order saddle point. The lowest-energy arrangement of the protonated 1-sulfanyl-3-propanal radical (-8.0 kJ mol<sup>-1</sup>) has the alcoholic proton syn to the carbon framework and the thiolic proton anti to it and requires 25.4 kJ mol<sup>-1</sup> in order to undergo the 1,2-shift. For further details regarding the various conformational aspects of this system, see Supporting Information.



the parent 3-propanal radical. The energy of the transition structure for the 1,2-shift (**TS:4**→**4'**) is lowered by 850.0 kJ mol<sup>-1</sup> upon protonation, some 25 kJ mol<sup>-1</sup> more than its unsubstituted counterpart. This result implies that the effect of protonation on reaction 4 should be even more dramatic than in the case of the 3-propanal radical. Indeed, protonation of the carbonyl oxygen in the sulfanyl-substituted system is found to lower the barrier for the intramolecular 1,2-shift by 60.9 kJ mol<sup>-1</sup> (the difference in the above proton affinities) to only 19.0 kJ mol<sup>-1</sup>.<sup>51</sup> For the reasons discussed earlier, protonation (or part thereof) could reasonably be expected to disfavor the fragmentation–recombination pathway.

Not surprisingly, the interaction of ammonium with the 1-sulfanyl-3-propanal radical is found to represent a situation intermediate between no protonation and full protonation. The size of the system that incorporates ammonium causes the CBS-RAD(p) calculations to become impractical. However, G2-(MP2,SVP)-RAD(p) predicts the barrier for the partially protonated 1,2-shift of the COSH group to be 63.5 kJ mol<sup>-1</sup>.<sup>52</sup>

The adequacy of replacing CoA by a hydrogen atom was tested by calculations employing a methyl group bonded to the sulfur atom. The calculated barriers (G2(MP2,SVP)-RAD(p)) for fragmentation–recombination (92.5 kJ mol<sup>-1</sup>), the concerted shift (85.7 kJ mol<sup>-1</sup>), and protonation–deprotonation (38.3 kJ mol<sup>-1</sup>) for the 1-methylthio-3-propanal radical suggest that the hydrogen atom is an adequate model for an alkyl chain and, hence, CoA in the current context.

The three theoretical techniques employed continue to demonstrate good agreement with one another (Table 2) for the species involved in Scheme 2. This level of consistency lends significant confidence to the use of the less expensive techniques for the quantitative evaluation of larger systems, such as those shown in reaction 5.

**D. (*R*)-Methylmalonyl-Related (5) to Succinyl-Derived (6) Radical Rearrangement.** The theoretical investigation of the model systems presented thus far provides valuable insight into the fundamental aspects of the rearrangements, as well as allowing much faster evaluation of properties of interest. However, there are two important aspects neglected by this approach, namely the exothermicity of the forward reaction in the more complete model (i.e., reaction 5) and the stereochemical aspects of the rearrangement.

For our largest and most realistic model of the enzymatic rearrangement, we have chosen the system shown in reaction 5 (see Scheme 3). The neutral carboxylic acid substituent is chosen in place of a charged carboxylate group to reflect the small net charge likely to be associated with the binding of this region by an arginine residue. A similar approach was employed in our treatment of the reaction catalyzed by 2-methyleneglutarate mutase<sup>17</sup> and seems justified by the finding of exactly this binding motif in the methylmalonyl-CoA mutase crystal structures<sup>2b</sup> (see also Section E). We continue to use a hydrogen atom in place of CoA as justified above. This same model system (reaction 5) has been investigated previously, using

(52) The conformational situation in the partially protonated 1-sulfanyl-3-propanal radical (**4-NH<sub>4</sub><sup>+</sup>**) is qualitatively very similar to that described for the fully protonated version.<sup>51</sup> If the conformer with both moieties anti to the carbon framework is assigned as 0.0 kJ mol<sup>-1</sup>,<sup>36</sup> the two enantiomeric first-order saddle points are calculated to be 47.9 kJ mol<sup>-1</sup> (G2(MP2, SVP)-RAD(p)) higher in energy, while the symmetric second-order saddle point (**TS:4-NH<sub>4</sub><sup>+</sup>→4'-NH<sub>4</sub><sup>+</sup>**) is found to be a further 15.6 kJ mol<sup>-1</sup> higher, at 63.5 kJ mol<sup>-1</sup>, which can again be viewed as an upper bound to the barrier for the overall process.<sup>51</sup> The lowest-energy conformer (−5.4 kJ mol<sup>-1</sup>) has the ammonium anti to the carbon framework and the thiolic proton syn to it and is connected to the reference zero-energy conformer by one of the C<sub>1</sub> transition structures at 47.9 kJ mol<sup>-1</sup>.

**Scheme 3.** Possible Mechanisms for the Rearrangement of the (*R*)-Methylmalonyl-Derived Radical (**5**) To Give the Succinyl-Related Radical (**6a**)

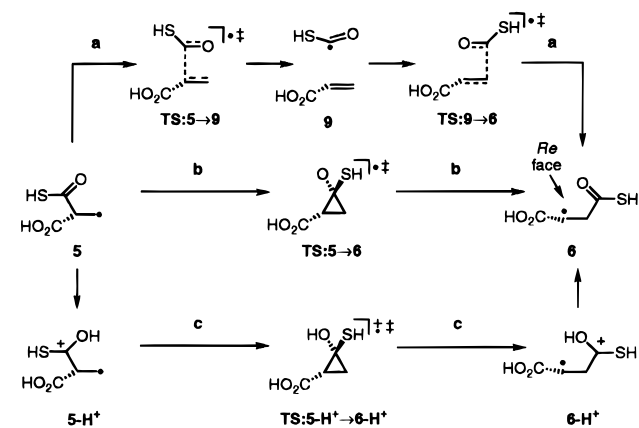


**Table 3.** Relative Energies (kJ mol<sup>-1</sup>)<sup>a</sup> of the Species Involved in the Rearrangement of the Methylmalonyl-Derived Radical (**5**) to the Succinyl-Related Radical (**6**) at 0 K

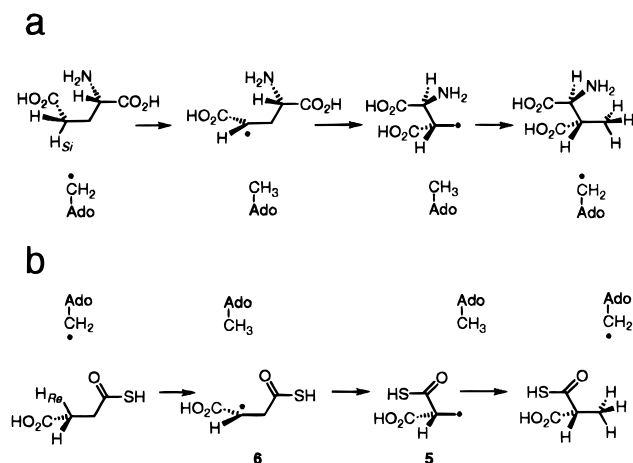
	G2(MP2,SVP)- RAD(p)	B3-LYP/ 6-31G(d,p)
methylmalonyl-derived radical ( <b>5</b> )	0.0	0.0
<b>TS:5</b> → <b>9</b>	71.5	64.1
sulfanylformyl radical + acrylic acid ( <b>9</b> )	52.6	39.8
<b>TS:9</b> → <b>9a</b>	74.1	67.8
<b>9a</b>	53.4	41.9
<b>TS:9a</b> → <b>6a</b>	62.2	49.9
<b>6a</b>	−32.5	−40.1
<b>TS:5</b> → <b>6</b>	64.3	63.7
succinyl-related radical ( <b>6</b> )	−29.9	−43.9
<b>TS:6</b> → <b>6a</b>	2.2	−4.9
<b>5-H<sup>+</sup></b>	0.0	0.0
<b>TS:5-H<sup>+</sup>→6-H<sup>+</sup></b>	33.0	20.3
<b>6-H<sup>+</sup></b>	−24.7	−42.3
<b>5-NH<sub>4</sub><sup>+</sup></b>		0.0
<b>TS:5-NH<sub>4</sub><sup>+</sup>→6-NH<sub>4</sub><sup>+</sup></b>		43.4
<b>6-NH<sub>4</sub><sup>+</sup></b>		−40.9
proton affinity of <b>5</b>	786.3	798.3
proton affinity of <b>TS:5</b> → <b>6</b>	817.6	841.6
proton affinity of <b>6</b>	781.1	796.7

<sup>a</sup> Energies relative to either **5**, **5-H<sup>+</sup>**, or **5-NH<sub>4</sub><sup>+</sup>**.

lower-level (Hartree–Fock and PM3) calculations.<sup>6d</sup> The results from that study indicated that the fragmentation–recombination mechanism (seemingly characterized only by the energy of the separated fragments at 62.9 (UHF) and 51.0 kJ mol<sup>-1</sup> (PM3)) is more favorable than the intramolecular migration (with barriers of 75.9 (UHF) and 139.7 (PM3) kJ mol<sup>-1</sup>). The radical rearrangement was found to be exothermic by 48.9 (UHF) and 31.8 (PM3) kJ mol<sup>-1</sup>.

The G2(MP2,SVP)-RAD(p) calculations find reaction 5 to be exothermic by 26.8 kJ mol<sup>-1</sup> (Table 3).<sup>53</sup> B3-LYP/6-31G(d,p) predicts a somewhat larger exothermicity of 40.1 kJ mol<sup>-1</sup>, and the majority of the remaining energies at this level (see Table 3) show a similar, but relatively constant, discrepancy. The energetic preference for the succinyl-related species is considerably greater on the radical surface (reaction 5) than it is on the parent, closed-shell surface (reaction 1). That is, reaction 1 is calculated to be exothermic by only 5.9 kJ mol<sup>-1</sup>, a finding that is qualitatively consistent with the recently

(53) The succinyl-related radical **6** has several stable conformations. In keeping with our methodology for the previous systems,<sup>32,50</sup> we have used the C<sub>1</sub> conformer shown in Figure 5 for the bulk of the calculations involving this molecule. See also Figure 7 and the Supporting Information.

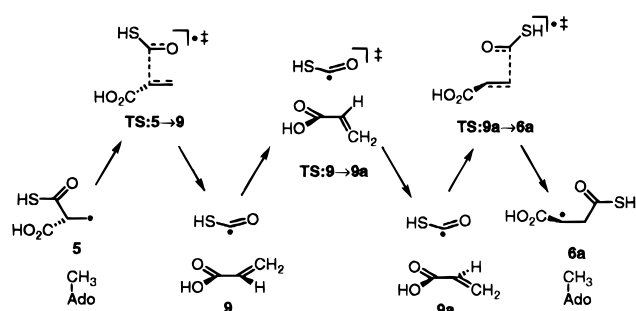
**Scheme 4.** Possible Rationalizations for (a) the Inversion Pathway of Glutamate Mutase and (b) the Retention Pathway of Methylmalonyl-CoA Mutase

calculated 20 kJ mol<sup>-1</sup> stabilizing effect of a carboxyl group at a radical center.<sup>30c</sup> The free energy ( $\Delta G$ ) of reaction 1 is calculated to be -8.9 kJ mol<sup>-1</sup> at 310 K, in good agreement with the  $\Delta G$  of -7.7 kJ mol<sup>-1</sup> derived from the experimental equilibrium constant ( $K = 0.05$ ).<sup>54</sup>

The stereochemistry of the methylmalonyl-CoA mutase reaction has been shown to involve specifically the (*R*)-isomer of methylmalonyl-CoA and the delivery of a hydrogen atom to the *Re* face of the product-related radical (see Scheme 3).<sup>15a,55</sup> That is, starting from succinyl-CoA, it is the *pro-R* hydrogen that is preferentially removed from C3 in the formation of **6**. Furthermore, considering the reaction in this direction (**6**→**5**), the hydrogen atom removed from C3 of succinyl CoA is replaced by the migrating group with retention of configuration. This contrasts with the stereochemical course of the other B<sub>12</sub>-dependent carbon skeleton mutases (glutamate mutase and 2-methyleneglutarate mutase), in which the migrating group replaces a neighboring hydrogen atom with inversion of configuration.<sup>56</sup>

For glutamate mutase, the inversion pathway can be rationalized<sup>15b,56</sup> by postulating the removal by the 5'-deoxyadenosyl radical of the *pro-S* hydrogen attached to C4 (H<sub>Si</sub> in Scheme 4a) of glutamate in a conformation in which this hydrogen atom is *anti* to the C2-C3 bond (see Scheme 4a). Indeed, this conformation for the substrate-derived radical (4-glutamyl) is in accord with EPR data.<sup>11</sup> Abstraction of this kind implies that the 5'-deoxyadenosine moiety is positioned on the opposite face of the molecule to the migrating group (in this case a glycol moiety). Following the migration, the product radical can receive a hydrogen atom from 5'-deoxyadenosine, the position of which has to change only slightly from that initially generated (see Scheme 4a). A similar argument can be presented for the 2-methyleneglutarate mutase-catalyzed rearrangement.<sup>56</sup>

The retention pathway of methylmalonyl-CoA mutase, however, requires a different explanation. One possibility is that the 5'-deoxyadenosyl radical appears on the same face of the molecule as the migrating group (Scheme 4b). In this arrangement, hydrogen abstraction from the substrate methyl group

**Scheme 5.** Pathway a of Scheme 3, Incorporating C-C Single Bond Rotation in Acrylic Acid for Stereochemical Consistency (See Also Figure 5)

allows the migration (of the formyl-CoA group) to occur with retention of configuration and delivery of the hydrogen atom to the *Re* face of the product-related radical as required (note that Scheme 4b shows the reaction in the reverse direction (**6**→**5**) for ease of comparison with glutamate mutase, Scheme 4a). There are, however, several steric impediments to this pathway. The migrating group and the 5'-deoxyadenosyl moiety would be positioned quite close to one another and would need to move directly past each other in their exchange of position. There are various possible adjustments that could alleviate some of the strain associated with this arrangement, but the crystal structure seemingly imposes an additional restriction. That is, a glutamine residue (Gln330) appears to be in a position that would limit the access of the hydrogen atom source to the upper face of the molecule (see section E).

Given the difficulties associated with a mechanism in which the 5'-deoxyadenosine moiety and the migrating group are positioned on the same side of the substrate, it is of interest to consider the stereochemical consequences of the 5'-deoxyadenosine moiety and the migrating group being on opposite sides of the substrate. This is additionally attractive, given the likelihood of such an arrangement in the other B<sub>12</sub>-dependent carbon skeleton mutases.<sup>56</sup> At initial inspection, it would seem that, if the reaction in Scheme 4b were drawn with the 5'-deoxyadenosyl radical below the substrate, then migration (regardless of the particular pathway) would be followed by delivery of the hydrogen atom to the *Si* face of C3, contrary to what is observed. There are, however, various possible internal rotations of the intermediates that can provide stereochemical consistency.

One such possibility lies within the fragmentation-recombination mechanism (pathway a, Scheme 3). Assuming that the substrate-derived radical **5** is formed by hydrogen abstraction from underneath (Scheme 5), the initial fragmentation is calculated to require 71.5 kJ mol<sup>-1</sup> (see Table 3). The two fragments (the sulfanylformyl radical plus acrylic acid or **9**) are predicted to lie 18.9 kJ mol<sup>-1</sup> lower than the initial transition structure (**TS:5**→**9**), or 52.6 kJ mol<sup>-1</sup> above the reactant. The most obvious motion that is able account for the observed stereochemistry is then a rotation about the C-C single bond in acrylic acid (i.e., **9**→**9a** in Scheme 5, initially suggested by Beatrix et al.<sup>15b</sup>). This motion, shown schematically in Scheme 5 but seen most clearly from the structures in Figure 5, disturbs the conjugation in the system and is predicted to require 74.1 kJ mol<sup>-1</sup> relative to the reactant (**5**), making it the rate-limiting step in this pathway. The two fragments may then recombine by addition of the sulfanylformyl radical at the more favorable  $\beta$ -position of the reorganized acrylic acid (via **TS:9a**→**6a** at 62.2 kJ mol<sup>-1</sup>) to form a rearranged conformation of product-related radical (**6a**) (at -26.8 kJ mol<sup>-1</sup>). Importantly, the *Re*

(54) Kellermeyer, R. W.; Alen, S. H. G.; Stjernholm, R.; Wood, H. G. *J. Biol. Chem.* **1964**, *239*, 2562-2569.

(55) (a) Michenfelder, M.; Hull, W. E.; Rétey, J. *Eur. J. Biochem.* **1987**, *168*, 659-667. (b) Hull, W. E.; Michenfelder, M.; Rétey, J. *Eur. J. Biochem.* **1988**, *173*, 191-201.

(56) Buckel, W.; Golding, B. T. *Chem. Soc. Rev.* **1996**, *26*, 329-337.



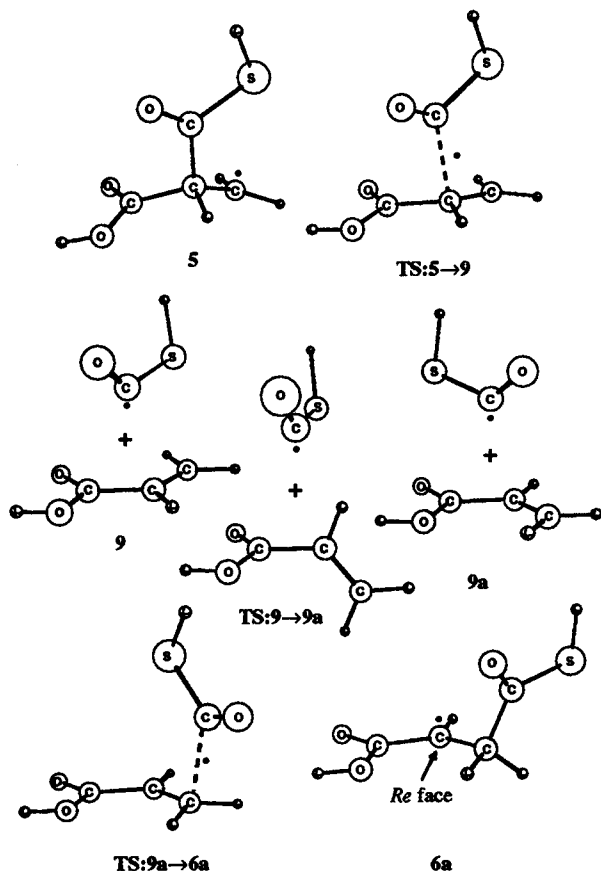


**Figure 5.** B3-LYP/6-31G(d,p) structures for the species involved in the fragmentation–recombination mechanism (Scheme 4) for the rearrangement of the methylmalonyl-derived radical (5).

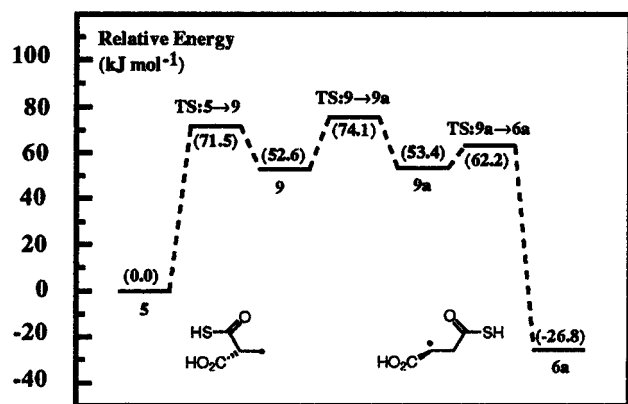


**Figure 6.** Schematic G2(MP2,SVP)-RAD(p) energy profile for the fragmentation–recombination pathway (Scheme 4) for the rearrangement of the methylmalonyl-derived radical (5). Relative energies ( $\text{kJ mol}^{-1}$ ) are shown in parentheses.

face of this conformer is now on the opposite side of the molecule to the migrating group (see Figure 5) and is, therefore, able to correctly receive a hydrogen atom from a molecule of 5-deoxyadenosine positioned *underneath* the substrate (Scheme 5). A schematic energy profile for this rearrangement pathway is shown in Figure 6.

Many textbooks<sup>57</sup> and much of the specialized literature<sup>4,6d</sup> show the mechanism of the radical rearrangement in the methylmalonyl-CoA mutase-catalyzed reaction as possibly

(57) See, for example: Bugg, T. *An Introduction to Enzyme and Coenzyme Chemistry*; Blackwell Scientific: Cambridge, MA, 1997; pp 210–211.

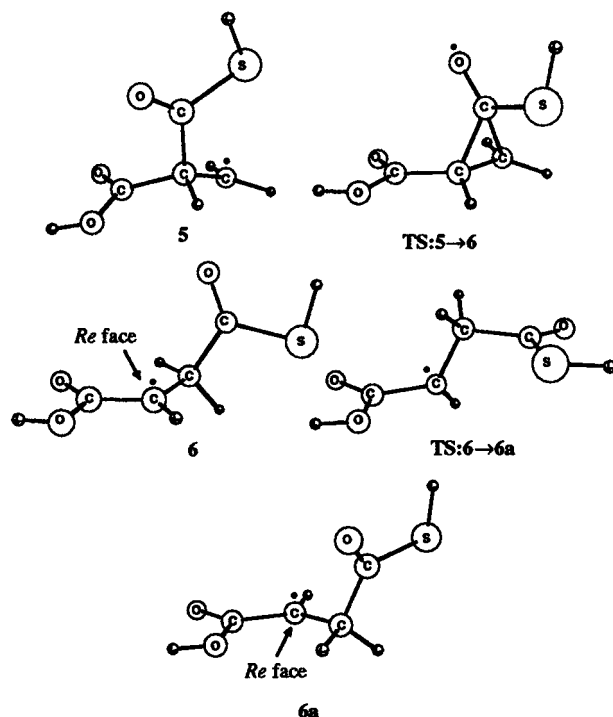


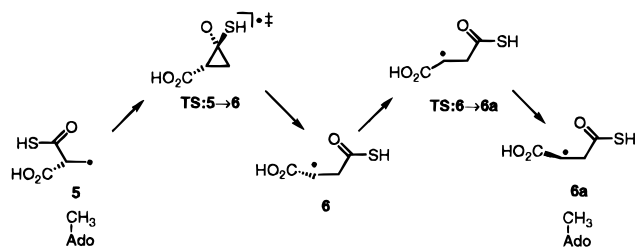
**Figure 7.** B3-LYP/6-31G(d,p) structures for the species involved in the intramolecular mechanism (Scheme 5) for the rearrangement of the methylmalonyl-derived radical (5).

occurring via a cyclopropyloxy intermediate (Scheme 3, pathway b). Although we find that this species corresponds to a transition structure rather than an intermediate (see below), it is instructive to consider the stereochemical consequences of this intramolecular pathway. As mentioned above, if the 5′-deoxyadenosine moiety is positioned underneath the substrate, any simple rearrangements of 5 would lead to a succinyl-related radical (6), which would accept a hydrogen atom with its *Si* face. There are, however, various distortions of the radical 6 that could convert it into the appropriate conformation (6a) for hydrogen atom delivery to the *Re* face (see Figure 7 for both structures). An important consideration is that both the carboxylic acid and the thioic S-acid groups may have quite restricted movement owing to their binding by the protein. That is, the carboxylic acid group is in close contact with Arg207, while the carbonyl oxygen of the thioic S-acid group is bound by His244 (see section E). The movement of the COSH group (COSCoA in the actual enzymatic reaction) would be additionally restricted by the covalent linkage between the sulfur atom and the remainder of the pantotheine chain. These restrictions would seem to indicate that a simple rotation of either group is unlikely. However, we find that it is possible for the central part of the molecule (the  $\text{CH}_2\text{—CH}^\bullet$  group) to “swing” from one side of the molecule to the other in a way that converts 6 into 6a without requiring large displacements in the two “anchoring” groups. As with the fragmentation–recombination pathway, a 5′-deoxyadenosine molecule positioned underneath 6a (Scheme 6) will then deliver a hydrogen atom to its *Re* face (Figure 7), in accord with experimental observation. Similar considerations apply to the intramolecular pathways involving full or partial protonation.

The motion in which the  $\text{CH}_2\text{—CH}^\bullet$  group is moved from one side of the molecule (as in 6) to the other (as in 6a) is

(58) The rotation directions are defined as if one were looking at a Fischer projection of the molecule with the rotating group in front and the remainder of the structure behind. If both rotations are defined from the same Fischer projection, then they are actually in the same direction.

**Scheme 6.** Pathway b of Scheme 3, Incorporating Internal Rotation in the Succinyl-Related Radical for Stereochemical Consistency



actually equivalent to a 180° anticlockwise rotation of the CO<sub>2</sub>H group, coupled with a 180° clockwise rotation of the COSH group.<sup>58</sup> Although this equivalence is difficult to picture, standard molecular models can provide significant aid. This twisting motion may be broken down into a series of discrete steps, where both groups have been twisted by small amounts (e.g., 30°) in opposite directions, thus allowing movement to occur in the central part of the molecule, while the two ends remain relatively fixed (as would be desirable for maintenance of binding to the protein). A relaxed potential energy scan constructed in exactly this way shows that the point of highest energy on such a coordinate is one where both groups have been twisted by approximately 90° with respect to the starting structure. This midpoint of the relaxed scan (**TS:6→6a**, see Figure 7) is predicted to lie 32.1 kJ mol<sup>-1</sup> above radical **6**.<sup>59</sup>

Given the energetic feasibility of this rotation within the product-derived radical (**6→6a**) and our earlier findings in the simpler model systems (reactions 3 and 4), it is certainly worthwhile to consider the energetics of the intramolecular rearrangements for reaction 5 (pathways b and c in Scheme 3). As mentioned briefly above, the species that resembles the 2-carboxy-1-sulfanylcyclopropoxy radical is found to be a transition structure (**TS:5→6**, see Figure 7) and not a local minimum.<sup>60</sup> This three-membered ring connects the (*R*)-methylmalonyl-derived radical (**5**) to the succinyl-related radical (**6**), and the reaction requires 64.3 kJ mol<sup>-1</sup> of energy in that direction. This rearrangement is exothermic by 29.9 kJ mol<sup>-1</sup>, implying that the twisting of **6** to **6a** can occur quite easily, requiring only slightly more energy (2.2 kJ mol<sup>-1</sup>) than that of the original substrate-derived radical and significantly less energy than the barrier for the initial migration (see Scheme 6

(59) In the absence of zero-point energy, the coupled rotation is predicted by B3-LYP/6-31G(d,p) to require 43.4 kJ mol<sup>-1</sup>. In support of the fact that this process is a combination of two rotations, we find that the rotation of the CO<sub>2</sub>H group alone requires 38.6 kJ mol<sup>-1</sup>, while the isolated rotation of the COSH requires only 1.0 kJ mol<sup>-1</sup>. We believe that our unsuccessful attempts to locate a second-order saddle point describing the coupled rotation are indicative not of its nonexistence but rather of the flatness of the potential for the COSH group rotation in the region of the CO<sub>2</sub>H rotation transition structure. As the maximum point on the relaxed scan is not strictly a stationary point, we obtained the zero-point energy contribution to the barrier as a combination of the contributions from the two isolated rotations (although as with the overall barrier, the zero-point contribution is almost exclusively derived from the CO<sub>2</sub>H rotation).

(60) Schemes 3 and 5 show **TS:5→6** to have the oxygen radical center and the carboxylic acid substituent be on the same side of the ring. There also exists a slightly higher energy (by less than 0.1 kJ mol<sup>-1</sup>) transition structure in which these two functional groups are on opposite sides of the ring. The X-ray crystal structure suggests that the biologically relevant arrangement is **TS:5→6**, as shown in Schemes 3 and 5. This same energy ordering for the two transition structures was also found in ref 6d.

(61) To prevent the additional proton from undergoing hydrogen-bonding interactions with the carboxylic acid group, it was constrained to be syn to the thiolic proton. This enables a more consistent comparison with the previous systems.<sup>36,51</sup> The resulting structures have converged (or virtually converged) energy gradients and are thus considered sufficiently close to the stationary points for the zero-point energies to be reasonable.

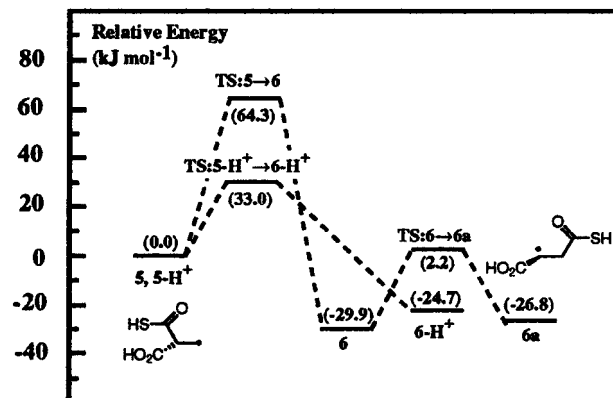


**Figure 8.** Schematic G2(MP2,SVP)-RAD(p) energy profile for the intramolecular pathway (Scheme 5) for the rearrangement of the methylmalonyl-derived radical (**5**). Relative energies (kJ mol<sup>-1</sup>) are shown in parentheses.

and Figure 8). Protonation of the carbonyl oxygen of the migrating thioic S-acid group lowers the intramolecular migration barrier to just 33.0 kJ mol<sup>-1</sup>,<sup>61</sup> consistent with proton affinities of 786.3 and 817.6 kJ mol<sup>-1</sup> for the reactant and transition structure, respectively. Interaction of the ammonium ion with the carbonyl oxygen results, yet again, in a situation intermediate between the two extremes, with a calculated barrier for rearrangement of 43.4 kJ mol<sup>-1</sup>.<sup>62</sup>

The incorporation of the twisting motion (**6→6a**) into the mechanism allows for stereochemical consistency in both the fragmentation–recombination and intramolecular pathways, with the 5'-deoxyadenosine molecule positioned anti to the migrating group (Schemes 5 and 6). The basic motion required in either pathway is the movement of a methylene group from one side of the active site to the other (see Figures 5 and 7). It may be that this adjustment is required to position the radical center better for hydrogen atom transfer. It has already been noted in the context of the fragmentation–recombination mechanism<sup>15b</sup> that occasional abstraction of H<sub>S</sub> from succinyl-CoA could explain the “error in the cryptic stereochemistry of methylmalonyl-CoA mutase”.<sup>15a,55</sup> That is, abstraction of H<sub>S</sub> would result in a conformation (**6**) whose rearrangement results directly in the correct stereochemistry of the substrate-derived radical (**5**), occasionally obviating the need for internal rotation within acrylic acid (**9→9a**).<sup>56</sup> Similarly, formation of **6** would bypass the internal twisting motion in the context of the intramolecular rearrangement. It should also be mentioned that it is not necessary for the methylene movement in the fragmentation–recombination mechanism to occur at the stage of separated fragments (**9**). Indeed it is energetically more favorable, even in the fragmentation–recombination pathway, for the twisting motion to occur at the stage of product-related radical (**6→6a**).<sup>63</sup>

Figure 9 combines the rearrangement possibilities discussed in this section. Pathway a(i) shows the fragmentation pathway

(62) For the same reason as outlined for the fully protonated rearrangement,<sup>61</sup> the ammonium ion was constrained to be syn to the thiolic proton (using the positions obtained from the 4-NH<sub>4</sub><sup>+</sup>→4-NH<sub>4</sub><sup>+</sup> rearrangement). In this instance, we have presented only the B3-LYP/6-31G(d,p) data (as G2(MP2,SVP)-RAD(p) calculations were computationally too demanding) and assumed that the zero-point contribution to the barrier is the same as in the 4-NH<sub>4</sub><sup>+</sup>→4-NH<sub>4</sub><sup>+</sup> rearrangement. For the zero-point contribution to the enthalpy, we used that obtained from the **5→6** rearrangement.

(63) For the recombination to occur in this way, a slightly different transition structure (**TS:9→6**) needs to be traversed. This transition structure is virtually the mirror image of **TS:9a→6a** (Figure 5). The latter is found (B3-LYP/6-31G(d,p)) to be less than 0.1 kJ mol<sup>-1</sup> lower in energy than the former. See Figure 9.

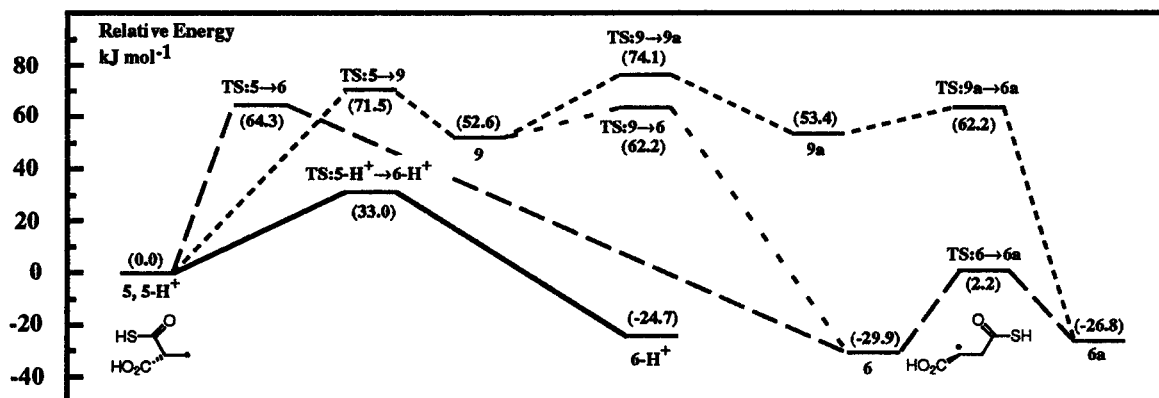


**Figure 9.** Schematic G2(MP2,SVP)-RAD(p) energy profile for the fragmentation–recombination (pathways a(i) (---) and a(ii) (- · - ·)) and intramolecular without protonation (pathway b (- · - ·)) and intramolecular with protonation (pathway c (—)) mechanisms for the rearrangement of the methylmalonyl-derived radical (5). Relative energies (kJ mol<sup>-1</sup>) are shown in parentheses.

with the stereochemical adjustment occurring at the separated fragment stage. Pathway a(ii) is the same basic mechanism except that the adjustment occurs within the product-derived radical. Pathways b and c correspond to the intramolecular migrations, without and with protonation, where TS:6→6a (or TS:6-H<sup>+</sup>→6a-H<sup>+</sup>) also needs to be traversed. Although the fragmentation–recombination mechanism cannot be ruled out on the basis of these data, the most likely possibility seems to be a proton-assisted intramolecular migration (such as 5-NH<sub>4</sub><sup>+</sup>→6-NH<sub>4</sub><sup>+</sup>), followed by a twisting of the product-related radical (6-NH<sub>4</sub><sup>+</sup>→6a-NH<sub>4</sub><sup>+</sup>).

**E. X-ray Crystal Structures.** Kinetic studies with <sup>3</sup>H-labeled 5'-deoxyadenosylcobalamin have shown that methylmalonyl-CoA mutase binds the coenzyme quite tightly.<sup>19</sup> The X-ray crystal structure data indicate that, in this holoenzyme form, the protein is in an open conformation, with a substrate-binding domain that is “split apart” and easily accessible to surrounding water.<sup>2b</sup> Upon substrate (or inhibitor) binding, the enzyme is seen to undergo a large conformational change as the CoA binding domain “closes up” around the substrate, burying the active site and rendering it largely inaccessible to solvent.<sup>2</sup> This sequestering of the active site from the surrounding medium is almost to be expected, given the highly reactive nature of the postulated radicals,<sup>64</sup> especially with respect to individual solvent molecules. Not only is this “dry” nature of the active site conducive to radical formation, but it also provides an ideal environment for partial proton transfer.

Figure 10 shows a small portion of the active site from the crystal structure of the mutant enzyme (Tyr89Phe) obtained with succinylcarbadethia-CoA as the substrate.<sup>3,65</sup> We have chosen this structure as all the other available Protein Data Bank files (relevant to methylmalonyl-CoA mutase) contain crystal structures which were obtained with inhibitors (e.g., 2- and 3-carboxypropyl-CoA) that lacked the migrating carbonyl group. In those cases, the active-site histidine (His244) is found to be somewhat displaced, attempting to donate a hydrogen bond to the carboxylic acid group. Although these structures indicate the willingness of this residue to act as a hydrogen bond donor, it would seem more appropriate to use a substrate equipped with the seemingly important carbonyl substituent in order to obtain a better representation of the true role of His244 in the active

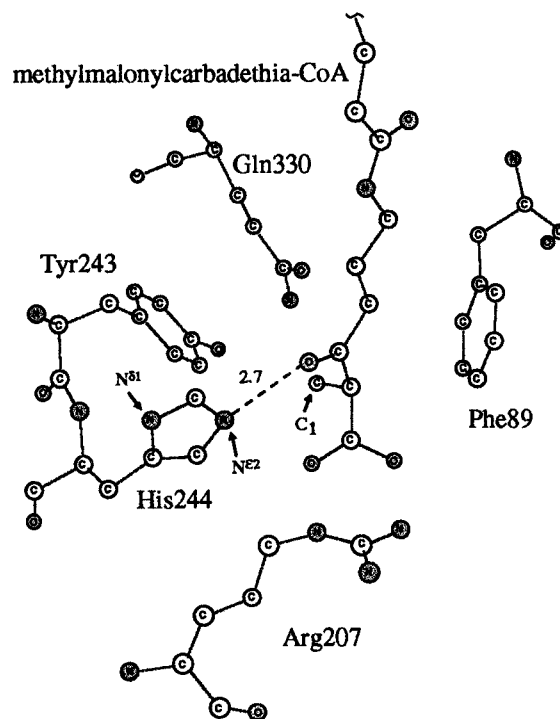


**Figure 10.** Small portion of the active site of the Tyr89Phe mutant of methylmalonyl-CoA mutase, taken from the Protein Data Bank.<sup>65</sup> Bond lengths are given in Å.

site of the wild-type enzyme. For clarity, we have only shown (2*R*)-methylmalonylcarbadethia-CoA, even though the crystal structure was determined by modeling the density as an equimolar mixture of this species and its rearranged counterpart, succinylcarbadethia-CoA. The close proximity of the histidine residue to the carbonyl group of the migrating group can clearly be seen. The distance between Nε<sup>2</sup> and the carbonyl oxygen is 2.7 Å in the crystal structure, remarkably similar to the N···O distance of 2.6 Å predicted in our model complex (5-NH<sub>4</sub><sup>+</sup>). Figure 10 also shows the close proximity of the arginine residue (Arg207) to the carboxylic acid substituent, as well as the restrictive position of Gln330 with respect to access to the upper face of the molecule by the 5'-deoxyadenosyl moiety.

The combination of the X-ray crystal structure and our calculations suggests that His244 could well provide partial protonation for catalysis. While hydrogen bonding from a neutral form of the histidine side chain would accomplish this, the effect would be less pronounced than if the imidazole ring were in its protonated form. However, even in the formally unprotonated

(64) Rétey, J. *Angew. Chem., Int. Ed. Engl.* **1990**, *29*, 355–361.

(65) The PDB code for the structure shown in Figure 10 is 5req. For information on the Protein Data Bank, see: (a) Abola, E. E.; Sussman, J. L.; Prilusky, J.; Manning, N. O. In *Methods in Enzymology*; Carter, C. W., Jr., Sweet, R. M., Eds.; Academic Press: San Diego, CA, 1997; Vol. 277, pp 556–571. (b) Sussman, J. L.; Lin, D.; Jiang, J.; Manning, N. O.; Prilusky, J.; Ritter, O.; Abola, E. E. *Acta Crystallogr.* **1998**, *D54*, 1078–1084.



form, any hydrogen bond donation to  $N^{\delta 1}$  would serve to increase the acidity at  $N^{\epsilon 2}$  (somewhat similar to the effect thought to be at work in the catalytic triad of the serine proteases<sup>43c</sup>) and impart upon it a closer resemblance to the protonated form. In this connection, the crystal structure shows several possible candidates for such a relay effect. For example, the amide proton from the backbone section of His244 is well positioned ( $N\cdots N$  distance of 3.1 Å) to donate a hydrogen bond to  $N^{\delta 1}$ . Assistance could also come from a neighboring lysine residue (Lys202, the presence of which led the crystallographers to suggest that His244 was unprotonated<sup>66</sup>), although the protein would need to undergo a slight conformational change to accomplish this. Regardless of the relay mechanism, the closeness of  $N^{\epsilon 2}$  to the substrate carbonyl would tend to suggest a stronger interaction than would be expected if the ring were in its fully unprotonated form.

The two remaining residues (Tyr243 and Phe89 or Tyr89) in Figure 10 are equipped with aromatic side chains. It may well be that these groups are involved with the stereochemical outcome of the reaction, and it is of interest to speculate as to how this might arise. As mentioned above, if the 5'-deoxyadenosine moiety is positioned below the substrate (Schemes 5 and 6), a methylene group ( $C_1$  in Figure 10) must be moved from one side of the active site to the other during the radical rearrangement (most clearly seen from the structures in Figures 5 and 7). The two aromatic groups can be seen to "bracket" the substrate in such a way that small movements of the rings could quite possibly repel or attract this relatively flexible methylene group and provide a possible means by which to govern the stereochemistry.

### Concluding Remarks

Our calculations on reactions modeling the coenzyme- $B_{12}$ -dependent rearrangement catalyzed by methylmalonyl-CoA mutase indicate that the fragmentation–recombination mechanism (pathway a in Schemes 1–3) is energetically more expensive than the alternative intramolecular pathways (routes b and c). This preference is somewhat reduced on going from our simplest model (reaction 3) to the more complete models (as in reactions 4 and 5) but is, nevertheless, still present.

(66) Evans, P. R.; Mancia, F. In *Vitamin B<sub>12</sub> and B<sub>12</sub>-Proteins*; Krautler, B., Arigoni, D., Golding, B. T., Eds.; Wiley-VCH: Weinheim, 1998; pp 217–226.

Although our calculations do not rule out the fragmentation–recombination pathway, the relatively high barrier in the unperturbed system, coupled with the expected destabilizing influence of a strong hydrogen bond donor, would seem to suggest an alternative mechanism.

The intramolecular mechanism, which proceeds in a single step via a three-membered cyclic transition structure, is unequivocally facilitated by protonation. The reduction in the barrier associated with the protonation of the carbonyl oxygen ranges from 30 to 60  $\text{kJ mol}^{-1}$  in the model systems investigated. Although complete protonation of this weakly basic group is unlikely, we have shown how partial proton transfer can reap the rewards of this barrier lowering, without resorting to the extreme. The X-ray crystal structures support this mechanistic picture, with a histidine residue (His244) being found in an ideal position to participate in both binding and catalysis. Our results have also led us to suggest a new step in the rearrangement that is consistent with the experimentally observed stereochemistry.

We have used ammonium as our principal model to illustrate the partial-proton-transfer concept in the present study. However, the important general conclusion that emerges from this work is that there is a continuous middle ground operating between the extremes of full and no protonation and, as long as a reaction is facilitated by protonation, partial proton transfer will reduce the reaction barrier.

**Acknowledgment.** We gratefully acknowledge generous allocations of time on the Fujitsu VPP300 and SGI Power Challenge computers of the Australian National University Supercomputing Facility. We thank the British Council for the award to D.M.S. of a Partnerships for Excellence Postgraduate Bursary to study at the University of Newcastle upon Tyne and the Research School of Chemistry at the Australian National University for the provision of a Visiting Fellowship for B.T.G..

**Supporting Information Available:** CBS-RAD (Tables S1 and S2) and G2(MP2,SVP)-RAD(p) (Table S3) total energies, and GAUSSIAN 94 and GAUSSIAN 98 archive entries for the B3-LYP/6-31G(d,p) calculations for all relevant structures (Table S4) (PDF). This material is available free of charge via the Internet at <http://pubs.acs.org>.

JA991649A